Tidal Velocity Asymmetries and Bedload Transport in Shallow Embayments[a]

Virginia A. Fry[b] and David G. Aubrey

Woods Hole Oceanographic Institution, Woods Hole, MA 02543, U.S.A.

Received 15 March 1988 and in revised form 14 September 1989

Keywords: estuaries; tidal circulation; sediment transport; analytical techniques; numerical model

Tidal circulation can cause a net transport of sediment when the tidal velocity is asymmetric about a zero mean (flood or ebb dominant) and the sediment transport rate is related nonlinearly to velocity. The relationship between tidal elevation and velocity is elucidated here to permit determination from tide gauge data and sediment transport relations whether tidal asymmetry needs to be considered as a mechanism for net sediment transport in the embayment of interest. A relationship between elevation and velocity in a shallow water, nonlinear system is derived through the continuity equation and shown to be significantly different than the linear relation. Finite difference numerical solutions of the one-dimensional, shallow water nonlinear equations are compared to the continuity relation and are in agreement especially toward the landward end of the channel. Tide gauge data collected at the landward end of the embayment are most useful for predicting velocity asymmetries throughout a major portion of the embayment channel.

The ratio of flood-to-ebb bedload transport and its relation to an asymmetric tidal elevation has been determined for both the linear relation between elevation and velocity and the nonlinear relation. Results show that the ratio of flood-to-ebb bedload transport as calculated from the nonlinear relation between elevation and velocity is similar to the flood-to-ebb ratio calculated from the linear relation because of offsetting effects.

Introduction

An embayment whose circulation is controlled by tidal forcing can have a net transport of sediment if the tidal velocity residual is nonzero or if the velocity is asymmetric about the mean. Residual currents, expressed by the advective terms in the momentum equations, can be generated by tidal currents flowing past topographic features (Tee, 1976; Zimmerman, 1981) and by other mechanisms. A tidal velocity that is asymmetric about a zero mean may be flood or ebb dominant. Flood (ebb) dominance occurs when currents in the flood (ebb) direction are stronger but have a shorter duration than ebb (flood) currents. Tidal asymmetries along the U.S. east coast can be described by the super-position

[a]Contribution number 7212 of the Woods Hole Oceanographic Institution.
[b]Present address: U.S. Geological Survey, Woods Hole, MA 02543, U.S.A.

0272–7714/90/050453+21 $03.00/0

of a fundamental frequency, the M_2 tidal constituent (lunar semidiurnal), with its harmonics, particularly the first harmonic, M_4 (Boon & Byrne, 1981; Aubrey & Speer, 1985). A tidal velocity that is flood or ebb dominant may cause a net sediment transport if the transport rate is related nonlinearly to velocity. Aubrey (1986) has calculated the ratio of flood-to-ebb bedload sediment transport as a function of the degree of flood or ebb dominance and has shown that a tidal velocity asymmetry around a zero mean may cause a significant transport asymmetry.

The emphasis of this paper is to understand tidal velocity asymmetry, its relation to tidal elevation asymmetry, and the significance of the elevation asymmetry in terms of sediment transport. Aubrey and Speer (1985) have shown, from observations at Nauset Inlet, how the offshore astronomical tide becomes strongly distorted as it propagates into shallow estuarine systems. This study, along with its companion study (Speer & Aubrey, 1985) focussed on the distortion of tidal elevation within the estuary due to the system geometry and dissipation characteristics. In order to understand the implications of tidal elevation distortion on near-bed, suspended, and dissolved material transport, the relation between elevation and velocity must be understood. A relation between elevation and velocity will enable one to determine from tide gauge data and sediment transport relations, the relative importance of tidal distortion on sediment movement in the embayment of interest. Since it is easier to measure vertical tides than horizontal tides for long durations, this methodology would be cost-effective.

Tidal asymmetries have been studied previously by analysing the shallow water nonlinear equations. The nonlinear equations generally do not have an exact analytical solution; thus, they must be solved using other methods. Numerical modelling methods, commonly used to solve nonlinear equations, do not display the relationship between various parameters of a system as clearly as do analytical methods. Numerical models must be run many times to determine how the various parameters of a system affect the solution. Perturbation analysis has been used by Kreiss (1957), Gallagher and Munk (1971), and Kabbaj and Le Provost (1980) together with numerical methods to solve the tidally-forced shallow water equations. All of these investigations used initial equations that drop nonlinear terms of order (tidal amplitude/water depth) that are significant in our calculations. Speer and Aubrey (1985) and Friedrichs and Aubrey (1988) related channel geometry to elevation asymmetry through numerical solutions, while maintaining the full nonlinear terms.

A relationship between elevation and velocity in a nonlinear system is derived here through the continuity equation. Numerical solutions of the shallow water equations check the validity of this method. Results show that the nonlinear relation between velocity and elevation is significantly different from the linear relation. The ratio of flood-to-ebb bedload transport is calculated as a function of elevation asymmetry to exemplify the significance of tidal asymmetry in transporting sediment.

The degree of elevation and velocity asymmetry can be described by an amplitude ratio of the first even harmonic tidal period to its fundamental tidal period and their relative phases. For a limited interval of time, frequency combinations other than a fundamental and its even harmonic may cause a net transport, but averaged over the longer period of the beat frequency, net transport will be zero. Thus, although M_6 and M_{10} are common, energetic forced constituents in shallow water horizontal tides, they do not contribute to net sediment transport when integrated over a suitable time interval. The M_2 tidal period (12·42 h) is the common fundamental tide of interest with its first even harmonic, M_4 (6·21 h), but other fundamental and even harmonic tidal combinations can also be important. Defining the fundamental and the first even harmonic frequency constituents (sea surface or velocity) as

$$A_{M_2} = a_1\cos(\omega t - \theta_1)$$
$$A_{M_4} = a_2\cos(2\omega t - \theta_2)$$

the amplitude ratio and the phase difference can be written

$$\frac{M_4}{M_2} = \frac{a_2}{a_1}$$
$$\Delta\theta = \theta_2 - 2\theta_1.$$

In present notation, a subscript reveals whether the phase or amplitude relationship refers to sea surface elevation (elev) or velocity (vel). Flood dominance occurs when $\Delta\theta_{vel}$ is between 270° and 90° with maximum asymmetry at 0°; ebb dominance occurs when $\Delta\theta_{vel}$ is between 90° and 270° with maximum asymmetry at 180°. The closer the amplitude ratio is to 1, the greater the asymmetry. Examples of how the amplitude ratio and phase difference express a velocity asymmetry and how a velocity asymmetry causes a net bedload transport can be seen in Speer (1984), Speer and Aubrey (1985), or Fry (1987).

Shallow water equations

Speer and Aubrey (1985) have shown that despite the physical complexities of shallow estuarine systems, estuarine tidal response can be recovered from one-dimensional models. The one-dimensional equations are not used to describe a real system in total, but to give insight into one aspect of the problem. The problem that is being addressed here is whether tidal asymmetries arising from nonlinear processes, need to be considered as a possible mechanism for transporting sediment in an embayment of interest. Integration of the shallow water equations over depth and width yields
conservation of mass

$$\frac{\partial A}{\partial t} + \frac{\partial U}{\partial x} = 0 \qquad (1)$$

and conservation of momentum,

$$\frac{\partial U}{\partial t} = -gA\frac{\partial \eta}{\partial x} - \text{friction term} - \text{advective term} \qquad (2)$$

where $A(x,t)$ is the area of the channel, $U(x,t)$ is the volume flux averaged over depth and width of the channel, $\eta(x,t)$ is the elevation of free surface above mean sea level, g is the gravitational acceleration, t is time, and x is positive upchannel, origin at the estuary mouth.

These equations define motion in a channel (Figure 1) having width, b, mean depth, h, and length, L. The width, b, and area, A, are defined as

$$b = b_o + \beta(h + \eta)$$
$$A = b(h + \eta) = b_o(h + \eta) + \beta(h + \eta)^2 \qquad (3)$$

where β is the slope of the side walls (width/height) and b_o is the width of the channel bottom.

The channel studied here is open at the ocean end ($x = 0$) and closed at the landward end ($x = L$). For tidally forced circulation in an embayment, the boundary conditions are

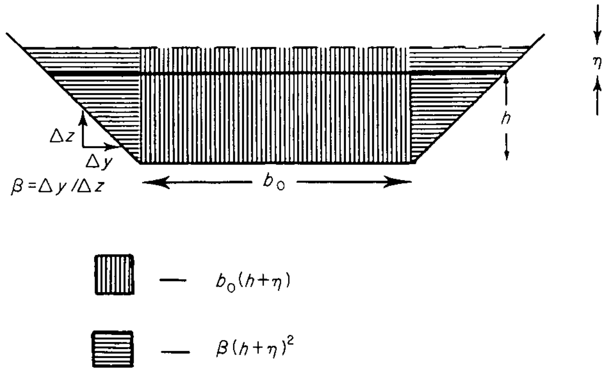

Figure 1. Channel geometry. The area of the channel that is marked by the vertical stippling is the area that changes in height only due to a change in tidal elevation. The horizontal stippling indicates the area of the channel that changes in both height and width due to a change in tidal elevation $\beta(h+\eta)^2$.

$$U = 0 \; at \; x = L \tag{4}$$

$$\eta = \eta_1 \cos(kL)\cos(\omega t) + \eta_2\cos(2kL)\cos(2\omega t - \theta) \; at \; x = 0 \tag{5}$$

where η_1 and η_2 are the amplitude of the fundamental and first harmonic frequency of elevation at the landward end of the channel ($x = L$), ω is the fundamental frequency, k is the wave number ($k = \omega/c, c = \sqrt{gh}$) and θ is the phase difference between the fundamental and harmonic frequency of the tidal elevation at the landward end of the channel ($x = L$).

Linear equations

The shallow water equations are linear if width, b, and area, A, are constant in space and time ($\eta/h \ll 1$), a linear friction term is used, and the nonlinear advective terms are neglected. In a linear system, an elevation asymmetry, and thus a velocity asymmetry, occur only when the system is being forced by both a fundamental and an even harmonic frequency [equation (5), $\eta_1 \neq 0$; $\eta_2 \neq 0$]. The elevation and velocity asymmetry for a linear solution with no friction are relatively simple. The amplitude ratio of the first harmonic to the fundamental frequency for velocity is approximately twice the amplitude ratio of the sea surface elevation, and the phase difference shows velocity is in quadrature with sea surface ($\Delta\theta_{vel} = \Delta\theta_{elev} + 90°$).

The solution to the linear equations with nonzero friction has been solved by Dronkers (1964). Dronkers' solution for velocity asymmetry, as related to elevation asymmetry, is more complex (Figure 2); quadrature is lost except near the landward end of the channel.

A linear system of the shallow water equations with and without friction shows the following relationship between velocity asymmetry and elevation asymmetry. The amplitude ratio of the first harmonic to the fundamental is

$$\frac{\mathrm{Amp}_{\mathrm{Harm,vel}}}{\mathrm{Amp}_{\mathrm{Fund,vel}}} \approx 2\left(\frac{\mathrm{Amp}_{\mathrm{Harm,elev}}}{\mathrm{Amp}_{\mathrm{Fund,elev}}}\right)_{x=L} = 2\frac{\eta_2}{\eta_1} \tag{6}$$

The phase relationship between the fundamental and the first harmonic is

$$\Delta\theta_{vel} = \Delta\theta_{elev,x=L} + 90° \tag{7}$$

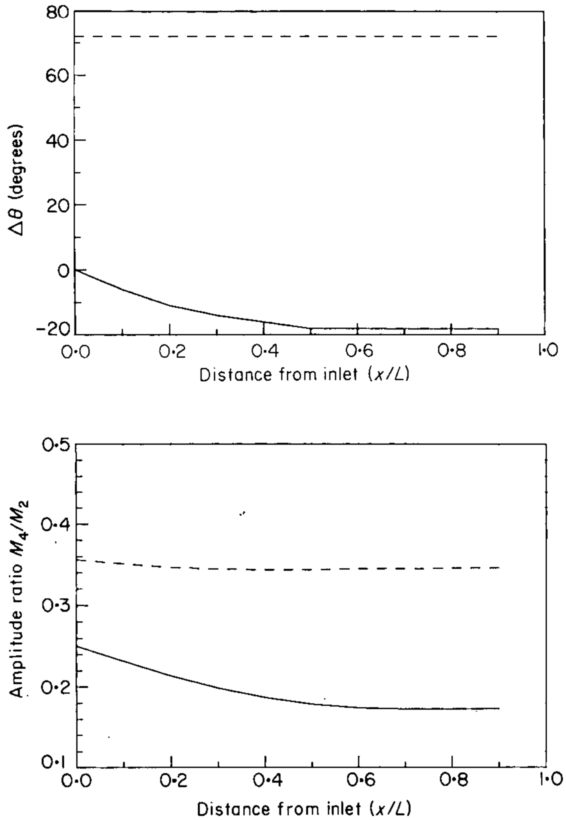

Figure 2. Comparisons between tidal elevation (——) and velocity (– – –) amplitude ratio and phase difference for a linear system with friction. ($h = 3{\cdot}0$ m, $L = 10$ km, $b_o = 50$ m, $\beta = 0$, $\mathrm{Amp}_{M_2,\mathrm{inlet,elev}} = 0{\cdot}8$, $\mathrm{Amp}_{M_4,\mathrm{inlet,elev}} = 0{\cdot}2$, $\Delta\theta_{\mathrm{inlet,elev}} = 0°$).

In linear solutions, velocity asymmetry varies insignificantly down the channel for a channel geometry on the order of 10 km in length and 3 m in depth (Figure 2). Linear solutions show that velocity asymmetry everywhere in the channel can be estimated well by the elevation asymmetry at the landward end of the channel.

Nonlinear equations

The shallow water equations [equations (1) and (2)] are nonlinear when area, A, or width, b, are not constant in time or space, or when the friction term and/or advection term is nonlinear. The nonlinear continuity equation is used to determine the relation between elevation and velocity asymmetry. Velocity is derived through the continuity equation using an elevation that is defined as a summation of tidal frequencies. Although the momentum equation is not used to determine the relationship between elevation and velocity asymmetry, the validity of this method will be evaluated by comparisons with numerical solutions.

The continuity solution is dependent on the existence of a tidal elevation that accurately predicts the velocity asymmetry for a major portion of the channel. In a linear system, a tidal elevation from the landward half of the channel can be used to predict accurately the velocity asymmetry everywhere in the channel (Figure 2). In a nonlinear system, tidal elevation data that can best estimate the velocity asymmetry throughout a major portion of the channel also comes from the landward end of the channel. This finding is verified by comparison with numerical solutions.

(i) *Continuity relation* Tidal velocity is determined from a tidal elevation that is characterized by a summation of harmonic frequencies

$$\eta = \eta_1\cos[k(x-L)]\cos(\omega t) + \eta_2\cos[2k(x-L)]\cos(2\omega t - \theta) \\ + \eta_3\cos[3k(x-L)]\cos(3\omega t - \zeta). \tag{8}$$

The second harmonic ($3\omega t$) is included in this expression because it is possible to create a first harmonic ($2\omega t$) from nonlinear terms creating interaction between the fundamental (ωt) and the second harmonic ($3\omega t$).

The velocity due to this elevation asymmetry is calculated from the volume flux, which is found using the continuity equation. A channel has an area that is expressed by equation (3) thus

$$\frac{\partial U}{\partial x} = -\frac{\partial A}{\partial t}$$

$$U = -(b_o + 2\beta h)\int \frac{\partial \eta}{\partial t}\,\mathrm{d}x - 2\beta\int \eta\frac{\partial \eta}{\partial t}\,\mathrm{d}x$$

$$U = (b_o + 2\beta h)\frac{\omega}{k}\left[\eta_1\sin[k(x-L)]\sin(\omega t) + \eta_2\sin[2k(x-L)]\sin(2\omega t - \theta)\right] \\ + \tfrac{1}{4}\beta\eta_1^2\frac{\omega}{k}\{2k(x-L) + \sin[2k(x-L)]\}\sin(2\omega t) + O(\eta_2\eta_1) + C$$

since $U=0$ at $x=L$, then $C=0$. The velocity is determined from the volume flux by

$$\text{Velocity} = V = U/A,$$

where

$$\frac{1}{A} = \frac{1}{b_o(h+\eta) + \beta(h+\eta)^2}.$$

Vertical side walls A channel having vertical side walls ($\beta=0$) simplifies the binomial expansion of $1/A$

$$\frac{1}{A} = \frac{1}{b_o h}\left[1 - \frac{\eta}{h} + O\left(\frac{\eta_1}{h}\right)^2\right].$$

$$V = \frac{\omega}{k}\frac{\eta_1}{h}\{\sin[k(x-L)]\sin(\omega t) + (\eta_2/\eta_1)\sin[2k(x-L)]\sin(2\omega t - \theta) \\ - (\eta_1/4h)\sin[2k(x-L)]\sin(2\omega t) + O[(\eta_1/h)^2] + O(\eta_2/h)\}$$

Two sinusoidal functions having the same frequency but different amplitudes and phases can be expressed as a single function of the same frequency with one amplitude and phase.

$$F\sin(2\omega t) + G\sin(2\omega t - \theta) = (F + G\cos\theta)\sin(2\omega t) - (G\sin\theta)\cos(2\omega t) \\ = [F + G\cos\theta)^2 + (G\sin\theta)^2]^{\frac{1}{2}}\sin(2\omega t - \varphi) \tag{9}$$

where

$$\varphi = \arctan\left(\frac{F + G\cos\theta}{-G\sin\theta}\right) - 90^\circ. \tag{10}$$

Thus,

$$V = \frac{\omega}{k}\frac{\eta_1}{h}\{\sin[k(x - L)]\sin(\omega t) + \left[\left(\frac{\eta_2}{\eta_1}\cos\theta - \frac{\eta_1}{4h}\right)^2 + \left(\frac{\eta_2}{\eta_1}\sin\theta\right)^2\right]^{\frac{1}{2}}$$
$$\sin[2k(x - L)]\sin(2\omega t - \varphi) + O[(\eta_1/h)^2] + O(\eta_2/h)\} \tag{11}$$

where

$$\varphi = \arctan\left(\frac{\dfrac{\eta_2}{\eta_1}\cos\theta - \dfrac{\eta_1}{4h}}{-\dfrac{\eta_2}{\eta_1}\sin\theta}\right) - 90^\circ.$$

The velocity asymmetry for a nonlinear system in a channel having vertical side walls is represented by the following equations. The amplitude ratio of the first harmonic (H_1) to the fundamental (F) is

$$\frac{\mathrm{Amp}_{\mathrm{H_1,vel}}}{\mathrm{Amp}_{\mathrm{F,vel}}} = \frac{\sin[2k(x - L)]}{\sin[k(x - L)]}\left[\left(\frac{\eta_2}{\eta_1}\cos\theta - \frac{\eta_1}{4h}\right)^2 + \left(\frac{\eta_2}{\eta_1}\sin\theta\right)^2\right]^{\frac{1}{2}}$$
$$\approx 2\left[\left(\frac{\eta_2}{\eta_1}\cos\theta - \frac{\eta_1}{4h}\right)^2 + \left(\frac{\eta_2}{\eta_1}\sin\theta\right)^2\right]^{\frac{1}{2}}. \tag{12}$$

The phase relationship between the fundamental and the first harmonic in the velocity equation when velocity is expressed as a summation of sine functions is

$$\Delta\theta_{\mathrm{vel}} = \theta_{H_1,\mathrm{vel}} - 2\theta_{F,\mathrm{vel}} + 90^\circ.$$

Thus,

$$\Delta\theta_{\mathrm{vel}} = \arctan\left(\frac{\dfrac{\eta_2}{\eta_1}\cos\theta - \dfrac{\eta_1}{4h}}{-\dfrac{\eta_2}{\eta_1}\sin\theta}\right).$$

But

$$\tan(180^\circ + A) = \tan(A),$$
$$\arctan(\,) = 180^\circ + A \text{ or } A,$$

therefore,

$$\Delta\theta_{\mathrm{vel}} = \arctan\left(\frac{\dfrac{\eta_2}{\eta_1}\cos\theta - \dfrac{\eta_1}{4h}}{-\dfrac{\eta_2}{\eta_1}\sin\theta}\right) + 0^\circ \text{ or } 180^\circ. \tag{13}$$

Choose 0° or 180° so $\Delta\theta_{vel}$ lags $\Delta\theta_{elev}$ in phase by approximately 90°. The amplitude ratio and phase relationship approaches the linear solution as $\eta_1/4h \rightarrow 0$.

Sloping side walls A v-shaped channel ($b_o = 0$) also simplifies the expansion of $1/A$ and therefore the calculation of the velocity as shown in the following equations

$$\frac{1}{A} = \frac{1}{\beta h^2}\left\{1 - \frac{2\eta}{h} + O\left[\left(\frac{\eta_1}{h}\right)^2\right]\right\}.$$

But $V = U/A$, so

$$\begin{aligned} V = {} & 2(\omega/k)(\eta_1/h)\{\sin[k(x-L)]\sin(\omega t) + (\eta_2/\eta_1)\sin[2k(x-L)]\sin(\omega t - \theta) \\ & + (\eta_1/8h)[2k(x-L)]\sin(2\omega t) \\ & - 3(\eta_1/8h)\sin[2k(x-L)]\sin(2\omega t) + O(\eta_2/h) + O[(\eta_1/h)^2]\}. \end{aligned}$$

The terms with the same frequency but different amplitudes and phases are combined using equations (9) and (10).

The velocity asymmetry for a nonlinear system with sloping side walls is represented by the following equations. The amplitude ratio of the first harmonic (H_1) to the fundamental (F) is

$$\frac{\mathrm{Amp}_{H_1,\mathrm{vel}}}{\mathrm{Amp}_{F,\mathrm{vel}}} = \frac{\sin[2k(x-L)]}{\sin[k(x-L)]}\left[\left(\frac{\eta_2}{\eta_1}\cos\theta - \frac{3\eta_1}{8h} + \frac{1}{8}\frac{2k(x-L)\eta_1}{\sin[2k(x-L)]h}\right) + \left(\frac{\eta_2}{\eta_1}\sin\theta\right)^2\right]^{\frac{1}{2}}.$$

The phase relationship between the fundamental and the first harmonic is

$$\Delta\theta_{vel} = \arctan\left[\frac{\dfrac{\eta_2}{\eta_1}\cos\theta - \dfrac{3\eta_1}{8h} + \dfrac{2k(x-L)\eta_1}{8\sin[2k(x-L)]h}}{-\dfrac{\eta_2}{\eta_1}\sin\theta}\right].$$

$$+0° \text{ or } 180°.$$

Choose 0° or 180° so that $\Delta\theta_{vel}$ lags $\Delta\theta_{elev}$ in phase by approximately 90°.

The velocity asymmetry determined for a v-shaped channel geometry is similar to the solution for a rectangular channel. A difference between the two solutions exists when $2k(x-L) \neq \sin[2k(x-L)]$. This difference is small for channel lengths much less than the tidal wavelength, as is true for the channels considered here.

Channels having geometries that are not rectangular or v-shaped but lie in between (i.e. flat bottom with sloping side walls) are more likely to be found in the field. Determination of the velocity asymmetry for a channel having a flat bottom and sloping sides becomes more difficult mathematically due to the binomial expansion of 1/area, where

$$\mathrm{Area} = b_0(h+\eta) + \beta(h+\eta)^2.$$

The relation between elevation and velocity asymmetry for geometries between a rectangular and v-shaped channel will be shown through numerical solutions in the section comparing numerical and theoretical results.

(ii) *Numerical method* The validity of the theoretical solutions will be checked by a comparison with numerical solutions. The nonlinear shallow water equations [equations

(1) and (2)] were solved numerically neglecting the advective term and using a quadratic friction term in the momentum equation

$$\text{friction term} = \frac{f|U|UP}{A^2}$$

where f is the dimensionless friction factor and P is the wetted perimeter ($P = b_o + 2[\beta^2(h+\eta)^2 + (h+\eta)^2]^{1/2}$).

A numerical solution of the nonlinear equations is found via an explicit finite difference model using a forward-time, centred-space scheme (Speer, 1984). Sea surface elevation and volume flux are staggered spatially. The accuracy of this scheme is $O(\Delta t, \Delta x^2)$. The equations in their discrete form are

$$\frac{\partial A}{\partial t} + \frac{\partial U}{\partial x} = 0$$

$$\frac{\partial \eta}{\partial t} + \frac{1}{b_o + 2\beta(h+\eta)}\frac{\partial U}{\partial x} = 0$$

$$\frac{\eta^{n+1}_{j+1/2} - \eta^{n}_{j+1/2}}{\Delta t} = -\frac{1}{b_o + 2\beta(h+\eta)^n_{j+1/2}}\frac{\mathrm{U}^n_{j+1} - \mathrm{U}^n_j}{\Delta x}$$

$$\frac{\partial U}{\partial t} = -gA\frac{\partial \eta}{\partial X} - \frac{f|U|UP}{A \cdot A}$$

$$\frac{U^{n+1}_j - \mathrm{U}^n_j}{\Delta t} = -gA^{n+1}_j\frac{\eta^{n+1}_{j+1/2} - \eta^{n+1}_{j-1/2}}{\Delta x} - \frac{f|U^n_j|U^n_jP^n_j}{A^n_j \cdot \mathrm{A}^n_j}.$$

The boundary conditions include a condition of no flux into solid boundaries,

$$U = 0 \text{ at } x = L,$$

and a forcing at the open channel boundary,

$$\eta = \eta_1 \cos(kL)\cos(\omega t) \text{ at } x = 0.$$

The analytical solution to the linear equations with no friction will be used for the initial conditions

$$\eta = \eta_1 \cos[k(x-L)] \text{ at } t = 0$$
$$U = 0 \text{ at } t = 0.$$

Tidal simulations are repeated for a number of cycles to ensure the solutions are independent of initial conditions. The stability criterion for the linearized numerical problem is the CFL condition (Roache, 1972)

$$\frac{\Delta x}{\Delta t} > \sqrt{gh_{\max}}$$

This condition is met by using $\Delta x = 250$ m and $\Delta t = 30$ s. The accuracy and stability of this numerical model are discussed in Speer (1984).

Time series of 5 days' duration for elevation, volume flux and velocity are calculated using the above equations. The first day is not included in the analysis to minimize transients. The amplitude and phase of the tidal elevation and velocity are determined using least squares harmonic analysis (Boon & Kiley, 1978; Aubrey & Speer, 1985).

Continuity versus numerical solutions The accuracy of the continuity approximation in determining the relation between elevation and velocity in the shallow water nonlinear equations is shown by comparisons with numerical solutions. Two channel shapes, rectangular and v-shaped, are used to show the comparisons between the linear, the nonlinear continuity and the nonlinear numerical solutions (Figures 3 and 4). These channel shapes have a similar channel area, but the wetted perimeter of the v-shaped channel is much greater. The nonlinear numerical solution of the velocity asymmetry is significantly different from the linear solution in both channel shapes; the rectangular channel is more nonlinear than the v-shaped channel. The v-shaped channel, having a larger wetted perimeter than the rectangular channel, has greater friction which decreases η_1/h. The degree of nonlinearity in the system is determined by η_1/h.

The velocity asymmetry calculated from the continuity relation best approximates the velocity asymmetry at the landward half of the channel as predicted by the numerical solutions. The continuity solution takes into account all the nonlinear terms in the equations of motion that would cause a nonlinear relation between elevation and velocity at the channel end. But the nonlinear variations along the channel are not represented. Nonlinear frictional effects increase with velocity and thus will increase toward the inlet, contributing to the along-channel variation in velocity asymmetry. The continuity solution determines a phase of the tidal velocity asymmetry that does not vary significantly from the numerical solution throughout most of the channel (Figure 3). The numerical solution of the amplitude ratio of harmonic to fundamental frequency decreases more than the continuity solution toward the inlet (Figure 4). The velocity asymmetry of the rectangular channel is represented better by the continuity solution than the velocity asymmetry of the v-shaped channel. Increased friction in the v-shaped channel also causes larger variations in elevation and velocity along the channel, which the continuity solution does not represent.

The velocity asymmetry determined from numerical solutions decreases towards the inlet as the amplitude ratio of harmonic to fundamental decreases and as the phase difference between fundamental and harmonic ($\Delta\theta_{vel}$) tends away from 0°. The velocity asymmetry generally decreases towards the inlet for the channel geometries examined here. If the numerical solution is assumed to be the 'true' solution, the tidal velocity asymmetry calculated from the continuity method is an upper limit for the asymmetry and hence also the sediment transport in the inlet due to this asymmetry.

Unfortunately, rectangular and v-shaped channels are not found commonly in the field. Channels having flat bottoms and sloping side walls are more realistic. Since the relation between velocity and elevation is difficult to determine analytically for these cases, it is shown by comparisons with numerical solutions that the continuity relation for rectangular channels is also a good approximation for various channel geometries between the rectangular and v-shaped extremes. Figure 5 shows the linear, the nonlinear continuity, and the nonlinear numerical solutions of the velocity asymmetry for a channel shape midway between the two extremes. The difference between the linear and nonlinear solutions in the channel with a flat bottom and sloping sides lies between the difference as seen in the rectangular and v-shaped channels. This difference is due to a wetted perimeter

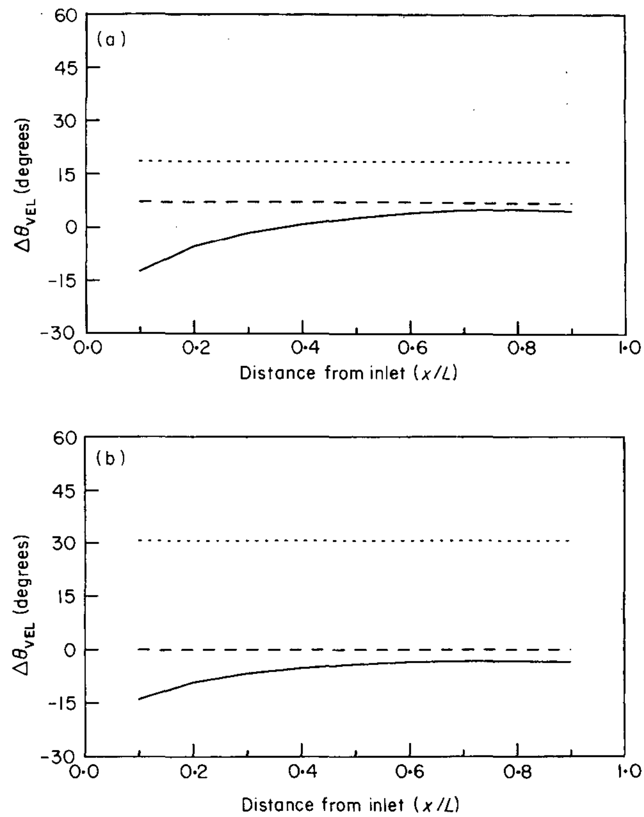

Figure 3. Comparisons of the tidal velocity phase differences for the numerical solution (——), the nonlinear continuity solution (– – –) and the linear solution (· · ·) for (a) a v-shaped channel ($b_o=0$, $\beta=20$) and (b) a rectangular channel ($b_o=50$ m, $\beta=0$) ($h=3{\cdot}0$ m, $L=10$ km, $f=0{\cdot}04$, $\mathrm{Amp}_{M_2,\mathrm{inlet,elev}}=0{\cdot}8\cos(kL)$, $Amp_{M_4,\mathrm{inlet,elev}}=0{\cdot}0$).

(and thus friction) that lies between those of the rectangular and v-shaped channels. The continuity solution predicts a phase difference that represents well the nonlinear numerical solution. The amplitude ratio at the landward end of the channel is also predicted well by the continuity solution. But the amplitude ratio at the inlet end of the channel as estimated by the continuity solution can only be used as an upper limit to the true asymmetry.

Numerical solutions show that tidal elevation at both the fundamental and harmonic frequencies reaches an amplitude half way down the channel that stays relatively constant to the end of the channel (Figure 6).Tide gauge data collected from any point in the landward half of the channel should provide the necessary input to determine the velocity asymmetry.

Near-bed sediment transport

Any sediment whose transport equation has a nonlinear relation to velocity may have a net transport in the flood or ebb direction if tidal velocity is composed of a fundamental

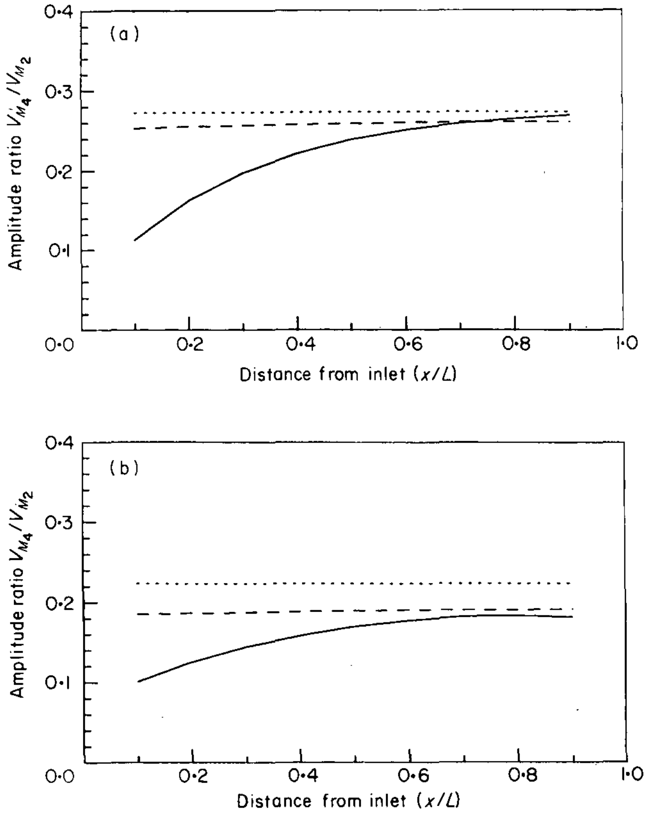

Figure 4. Comparisons of the tidal velocity amplitude ratio for the numerical solution (——), the nonlinear solution (– – –) and the linear solution (· · ·) for (a) a v-shaped channel ($b_o = 0, \beta = 20$) and (b) a rectangular channel ($b_o = 50$ m, $\beta = 0$). Same parameters as given in caption to Figure 3.

frequency and its even harmonic. The previous sections have shown how tidal velocity is estimated from tidal elevation data. The purpose of this section is to relate tidal elevation to net near-bed sediment transport due to an asymmetrical tide. This exercise will enable one to determine from tide gauge data whether tidal asymmetry needs to be considered as a mechanism for net near-bed sediment transport in an embayment of interest. The flood-to-ebb ratio of near-bed sediment transport can be calculated from a knowledge of the tidal velocity.

Bedload sediment transport has been expressed in a variety of ways. The Meyer-Peter and Müller bedload formula was derived from purely empirical relations (Meyer-Peter & Müller, 1948). The original equation has been changed by Wilson (1966) to include the Shield's parameter

$$q_{sb} = 8\left[d\sqrt{\left(\frac{\rho_s}{\rho} - 1\right)\rho g d}\right](\Psi - \Psi_c)^{3/2}$$

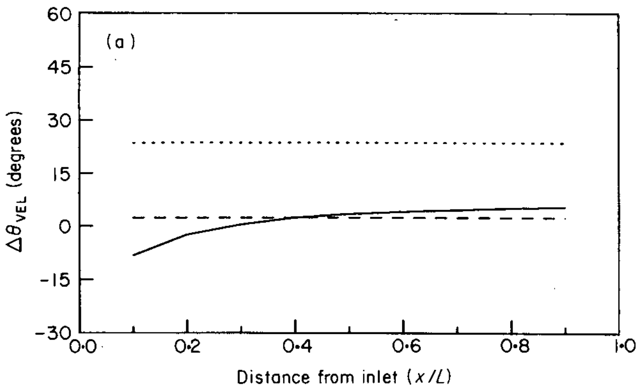

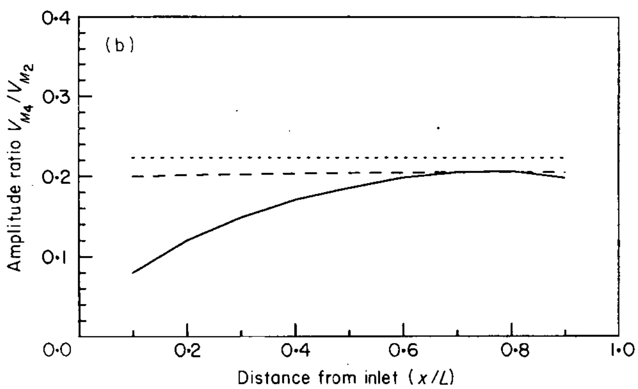

Figure 5. Comparisons of (a) the phase difference and (b) the amplitude ratio for velocity between the numerical solution (——), the nonlinear continuity solution (– – –) and the linear solution (· · ·) for a channel with a flat bottom and sloping side walls. ($h=3$ m, $L=$ 10 km, $f=0{\cdot}04$, $b_o=30$ m, $\beta=10$, $\mathrm{Amp}_{M_2,\mathrm{inlet,elev}}=0{\cdot}8\cos(kL)$, $\mathrm{Amp}_{M_4,\mathrm{inlet,elev}}=0{\cdot}0$).

where q_{sb} is volume rate of transport per unit width, Ψ is Shield's parameter, Ψ_c is critical Shield's parameter defining initiation of sediment movement, d is grain diameter, ρ_s is density of sediment, and ρ is density of water.

$$\Psi = \frac{\tau_o}{\left(\frac{\rho_s}{\rho} - 1\right)\rho g d}$$

$$\tau_o = u_*^2 \rho$$

$$u_* \propto \bar{u}$$

$$\tau_o \propto \bar{u}^2$$

where τ_o is shear stress, u_* is shear velocity, $\bar{u}$ is depth averaged velocity, and $\bar{u}_c$ is critical depth averaged velocity defining initiation of sediment movement. If $\Psi_c \neq 0$, then

$$q_{sb} \propto (\bar{u}^2 - \bar{u}_c^2)^{3/2}.$$

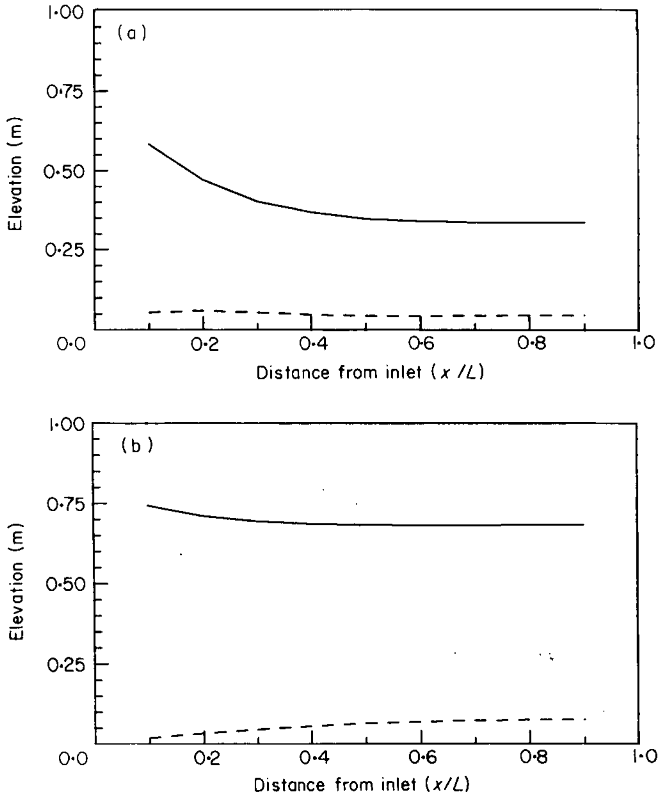

Figure 6. Numerical solution for the elevation amplitude of the fundamental (——), and harmonic frequencies (– – –) for (a) a v-shaped ($b_o = 0$, $\beta = 20$) and (b) a rectangular channel ($b_o = 50$ m, $\beta = 0$). Same parameters as given in caption to Figure 3.

If $\Psi_c = 0$, then

$$q_{sb} \propto \bar{u}^3.$$

The Meyer-Peter and Müller equation shows that bedload transport is proportional to velocity cubed. The Bagnold equation of bedload transport, which is based on the assumption that the volume of transport is proportional to the energy loss per unit area of the bed due to friction between the fluid and the bed, is also proportional to velocity cubed (Bagnold, 1963).

Aubrey (1986) calculated the relation between velocity asymmetry and the flood-to-ebb ratio using the Meyer-Peter and Müller formula with $\Psi_c = 0$. Elevation asymmetry for both linear and nonlinear systems now can be related to the flood-to-ebb ratio of bedload transport using the relationship between elevation and velocity asymmetry as calculated in the previous sections. The Meyer-Peter and Müller equation will be used for this analysis. By presenting the ratio of flood-to-ebb sediment transport, the need to specify the sediment parameters in the transport equation is eliminated. This information will allow a prediction of the ratio of flood-to-ebb bedload transport from knowledge of tidal elevation at the landward end of the channel.

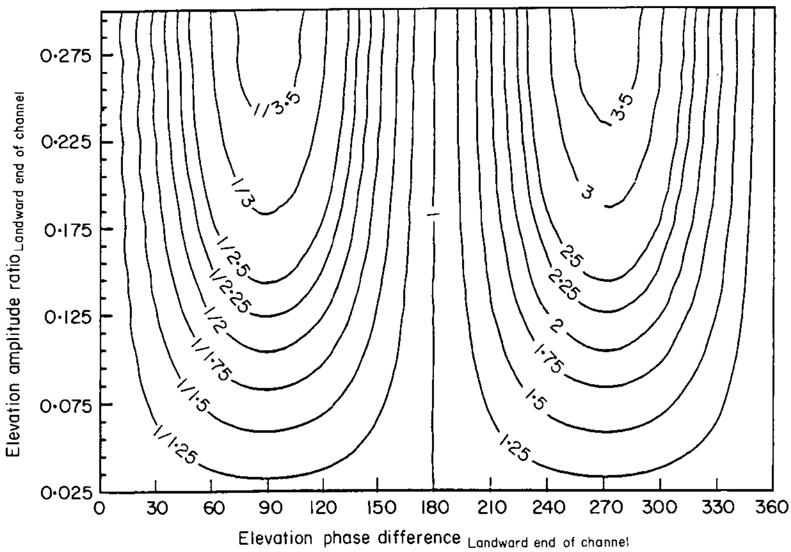

Figure 7. Tidal elevation asymmetry *vs.* flood-to-ebb ratio of bedload sediment transport. Velocity is linearly related to elevation, critical velocity is zero and the relation holds for the length of channel if the channel length is much less than the wavelength of the tide ($V_{crit} = 0$ cm s^{-1}).

The ratio of flood-to-ebb sediment transport is

$$\frac{\int_{\text{flood}} (\overline{u}^2 - \overline{u}_c^2)^{3/2} \mathrm{d}t}{\int_{\text{ebb}} (\overline{u}^2 - \overline{u}_c^2)^{3/2} \mathrm{d}t}$$

where $\overline{u}$ is derived from elevation information. The flood-to-ebb ratio of bedload transport is plotted *vs.* the elevation asymmetry of a linear system in Figure 7 [using equations (6) and (7)]. Phase differences of 0° and 180° in elevation will translate into a velocity that will not have a flood or ebb dominance: velocity still may be distorted but will be symmetrical between flood and ebb. The closer the amplitude ratio is to one, the more distorted the velocity becomes with potential for greater asymmetry and thus larger differences between flood and ebb transport.

A nonlinear system shows a flood-to-ebb ratio dependence on elevation asymmetry similar to that of the linear system [Figure 8, using equations (12) and (13) to relate elevation to velocity]. The nonlinear continuity solution for the amplitude ratio and the phase difference earlier were shown to be significantly different from the linear solution when η_1/h is not $\ll 1$. The differences between the nonlinear and the linear solutions for the velocity amplitude ratio and the phase difference cancel each other in the calculation of the flood-to-ebb transport ratio. These differences combine to predict a flood-to-ebb ratio that is along the isoline of the flood-to-ebb ratio as calculated in the linear solution.

This result can be shown best by Table 1 and Figure 9. Table 1 shows that when $\Delta\theta_{\text{elev}}$ is within 0–90° (ebb dominant), $\cos\theta$ is positive causing the nonlinear velocity amplitude

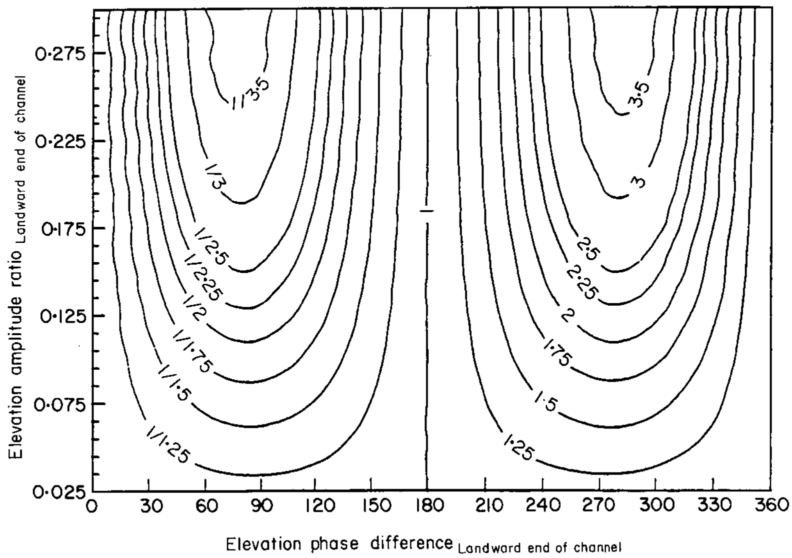

Figure 8. Tidal elevation asymmetry *vs.* flood-to-ebb ratio of bedload sediment transport. Velocity is nonlinearly related to elevation, critical velocity is zero and the relation holds for the length of channel if the channel length is much less than the wavelength of the tide ($\eta_1/h = 0{\cdot}3\ V_{crit} = 0\ \mathrm{cm\ s^{-1}}$).

TABLE 1. Differences between the linear and nonlinear relation between elevation and velocity, and their effect on the flood-to-ebb bedload transport ratio

$\Delta\theta_{elev}$	$\cos\theta$	$\dfrac{Amp_{H,vel}}{Amp_{F,vel\,NL}}$	Flood[a]/Ebb	$\Delta\theta_{vel}$— $\Delta\theta_{elev\,NL}$	$\Delta\theta_{vel,NL}$	Flood[b]/Ebb
0–90°	+	$\dfrac{<2\ AMP_{H,elev}}{AmpF,elev}$	↑	>90°	→180°	↓
90–180°	−	$\dfrac{>2\ AMP_{H,elev}}{AmpF,elev}$	↓	>90°	→0°	↑
180–270°	−	$\dfrac{>2\ AMP_{H,elev}}{AmpF,elev}$	↑	<90°	→180°	↓
270–360°	+	$\dfrac{<2\ AMP_{H,elev}}{AmpF,elev}$	↓	<90°	→0°	↑

[a]The change in the linear flood/ebb due to the nonlinear change in the amplitude.
[b]The change in the linear flood/ebb due to the nonlinear change in the phase difference.
(NL = nonlinear, ↑ = increases, ↓ = decreases, → = approaches.)

ratio to be less than that predicted by the linear relation [equation (12)]. A decrease in the velocity amplitude ratio by the nonlinear relation causes the system to become less ebb dominant, increasing the flood-to-ebb ratio. The vertical arrow in the 0–90° quadrant

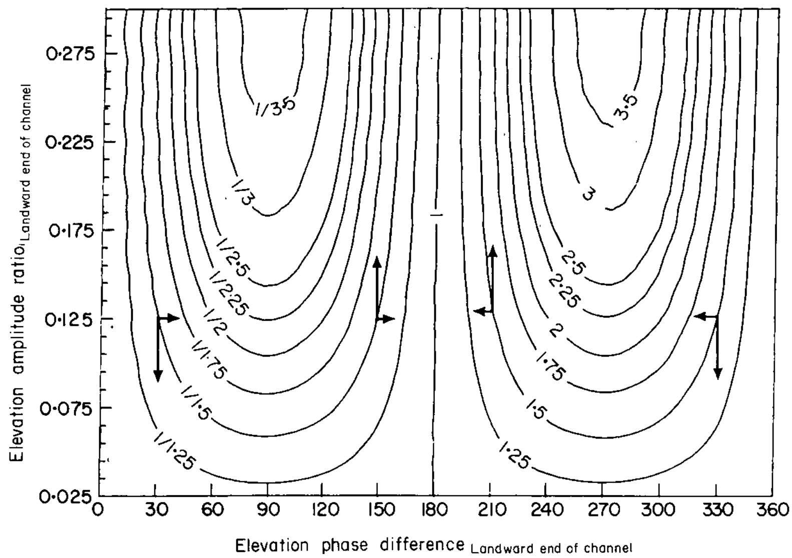

Figure 9. An illustration of how the difference between the nonlinear and the linear solutions for the velocity amplitude ratio and phase difference cancel each other in the calculation of the flood-to-ebb bedload transport ratio. Same parameters as given in caption to Figure 7.

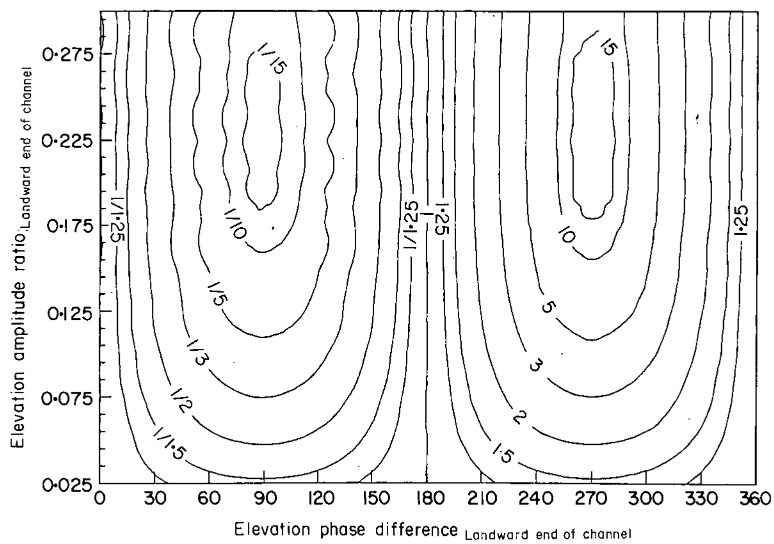

Figure 10. Tidal elevation asymmetry *vs.* flood-to-ebb ratio of bedload sediment transport, 2 km from the inlet. Velocity is linearly related to elevation, $V_{crit} = 20$ cm s^{-1}, $L = 10$ km, $h = 3$ m.

(Figure 9) represents the increase in the flood-to-ebb ratio due to the nonlinear velocity amplitude ratio. Table 1 and Figure 9 also show that when θ is between 0–90°, the phase difference between velocity and elevation is greater than 90° [equation (13)]. The $\Delta\theta_{elev}$ is

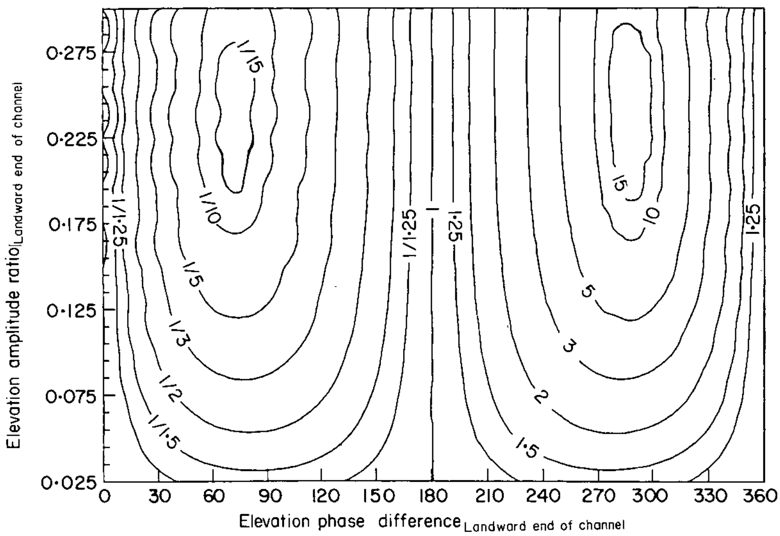

Figure 11. Tidal elevation asymmetry *vs.* flood-to-ebb ratio of bedload sediment transport 2 km from the inlet. Velocity is nonlinearly related to elevation, $V_{crit} = 20$ cm s^{-1}, $L = 10$ km, $h = 3$ m.

between 0–90°, thus the $\Delta\theta_{\text{vel}}$ is $90°^{+}$–$180°^{+}$. The $\Delta\theta_{\text{vel}}$ gets closer to 180° due to the nonlinear relation, the system becomes more ebb dominant, and the flood-to-ebb ratio decreases. The horizontal arrow in the 0–90° quadrangle (Figure 9) represents the decrease in the flood-to-ebb ratio due to the nonlinear phase difference. The remaining quadrants show similar behaviour.

For coarser sediments, the velocity has to reach a certain magnitude before initiation of sediment movement. Figure 10 shows the flood-to-ebb ratio of a linear system with a critical velocity of 20 cm s^{-1} ($\psi_c = 0{\cdot}12$, $u_* = 1{\cdot}17$ cm s^{-1}). This critical velocity corresponds to a fine sand with a grain size of 0·07 mm. A greater flood-to-ebb transport asymmetry occurs when sediment is stationary for part of the tidal cycle. A nonlinear system with a critical velocity of 20 cm s^{-1} (Figure 11) also shows flood-to-ebb ratios similar to the linear system.

Calculation of the flood-to-ebb ratio of bedload transport for a nonlinear system can be determined from the linear relation. Since other sediment transport relations may be related to velocity in different ways, the calculation of the nonlinear velocity may be required to determine the sediment transport. The flood-to-ebb transport ratios are calculated here based on the assumption that the continuity solution approximates the true solution adequately. The following section examines the error associated with the use of the continuity relation for sediment transport calculations.

Error determination

The relation between elevation and velocity determined from the continuity solution of the nonlinear equations is not identical to the numerical solution (Figures 3–5). The continuity and the numerical solutions predict the same nonlinear relation between

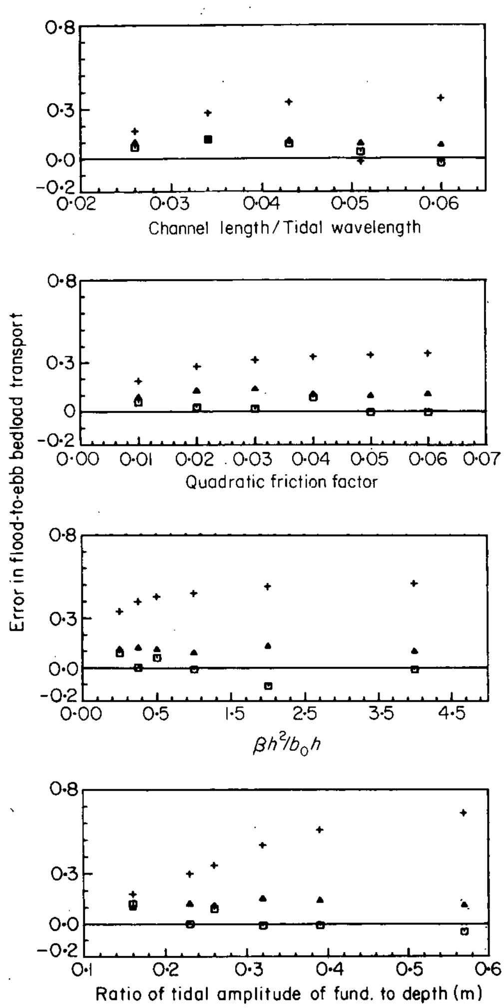

Figure 12. Error determination of the nonlinear continuity solution in terms of the ratio of flood-to-ebb bedload transport as a function of various parameters of the system and distance along channel [□, $x/L=0{\cdot}8$; Δ, $x/L=0{\cdot}5$; +, $x/L=0{\cdot}2$]. ($\mathrm{Amp}_{M_2,\mathrm{inlet,elev}}=0{\cdot}8\cos(kL)$, $\mathrm{Amp}_{M_4,\mathrm{inlet,elev}}=0{\cdot}0$, $h=3$ m, $L=10$ km, $b=50$ m, $\beta=0{\cdot}0$, $V_{crit}=0{\cdot}0$).

elevation and velocity at the landward end of the channel, but the velocity asymmetry along the channel, as predicted by numerical solutions, varies from the continuity solution increasingly toward the inlet. Numerical solutions show that most of the nonlinear variation along the channel occurs at the inlet end of the channel.

Estimates of the error in the continuity solution are defined by the difference between the continuity and numerical solutions for the flood-to-ebb bedload transport ratio. The error in the flood-to-ebb ratio of a nonlinear system is dependent on the parameters of the system and the distance down the channel (Figure 12). For channel geometries of interest here, the flood-to-ebb ratio of the continuity solution is similar to or greater than the numerical solution; their difference increases towards the inlet. As the system becomes more nonlinear, the error in the continuity solution at the inlet increases (Figure 12).

Conclusions

To understand sediment transport in estuaries and bays, the various processes that cause this transport must be discerned. Tidal asymmetry is just one means of transporting sediment in a bay or estuary. This paper has shown how to estimate from the vertical tide if there is a potential for net transport of sediment in a flood or ebb direction due to tidal asymmetries in the embayment of interest. The assumed geometry of the channel is extremely simple and there is no intent to model sediment transport in an estuary in its entirety. The idea here is to simplify all other aspects of the problem so one aspect can be examined solely and in detail. The primary conclusions are summarized below.

1. Numerical solutions of a simple channel show that the nonlinear relation between tidal elevation asymmetry and tidal velocity asymmetry is significantly different to the linear relation when η_1/h is not $\ll 1$. Tidal asymmetry is represented by the amplitude ratio and phase difference of a fundamental frequency and its first even harmonic.

2. The continuity equation is used to determine the relation between tidal elevation asymmetry and tidal velocity asymmetry. This method determines a direct relation between the parameters in the system and the relation between elevation and velocity asymmetry. The relations between tidal elevation and velocity asymmetry from channels having vertical side walls and sloping side walls are similar. The differences between the linear and nonlinear relation are dependent on $\eta_1/4h$ as seen in equations (12) and (13). The continuity solution uses tidal elevation information from gauges positioned at the landward half of the channel. The nonlinearities in the tide gauge data are generated by mechanisms represented in both the continuity and momentum equations. The nonlinear effects in the tidal elevation, most of which are developed near the inlet end of the channel, are then incorporated into the continuity solution.

3. The continuity solution is compared to numerical solutions and found to represent accurately the numerical solutions of the amplitude ratio at the landward half of the channel, but not as well near the inlet. The phase difference is approximated well throughout most of the channel, especially when the wetted perimeter is not large or friction is low.

4. The flood-to-ebb ratio of near-bed sediment transport is related to tidal elevation asymmetry using the continuity solution as an approximation of the relation between elevation and velocity asymmetry. This result is compared to the flood-to-ebb ratio using a linear relation between elevation and velocity asymmetry and found to give similar results. Although the nonlinear relation between elevation and velocity amplitude ratio and phase difference was found to be significantly different than the linear relation, combining the changes in the amplitude ratio and the phase difference cancelled out the nonlinear effects on the flood-to-ebb ratio of bedload sediment transport. This result is also true when a critical velocity of 20 cm s^{-1} is used.

5. An estimate of whether tidal asymmetry is important for transporting near-bed sediment in the embayment of interest can be found using the linear relation between tidal elevation and velocity. Tide-gauge data along with Figures 7 and 10 can be used for bounding the range of the flood-to-ebb ratio due to tidal velocity asymmetry. This estimate is valid in the landward half of the channel and represents an upper limit at the inlet end.

Acknowledgements

This work was sponsored by NOAA National Sea Grant College Program Office, Department of Commerce, under grant number NA86-AA-D-SG090, WHOI Sea Grant Project Number R/M-16-PD, by the U.S. Army Engineer Waterways Experiment Station's Coastal Engineering Research Center, (completed as part of the Inlet Channel work no. 31716 of the Harbor Entrance and Coastal Channels Program), by the Woods Hole Oceanographic Institution's Education Office, and by the Woods Hole Oceanographic Institution's Coastal Research Center. This article was reviewed by E. Uchupi and J. Trowbridge, as well as two external referees.

References

Aubrey, D. G. 1986 Hydrodynamic controls on sediment transport in well-mixed bays and estuaries. In: *Physics of Shallow Estuaries and Bays* (van de Kreeke, J., ed.). Berlin: Springer-Verlag, pp. 245–258.

Aubrey, D. G. & Speer, P. E. 1985 A study of non-linear tidal propagation in shallow inlet/estuarine systems. Part I: Observations. *Estuarine, Coastal and Shelf Science* **21**, 185–205.

Bagnold, P. A. 1963 Mechanics of marine sedimentation. In: *The Sea*, 3, (Hill, M. N., ed.). New York: Wiley, pp. 507–582.

Boon, J. D. III & Byrne, R. J. 1981 On basin hyposymmetry and the morphodynamic response of coastal inlet systems. *Marine Geology* **40**, 27–48.

Boon, J. D. III & Kiley, K. P. 1978 Harmonic analysis and tidal prediction by the method of least squares. Special report No. 186, Virginia Institute of Marine Science, Gloucester Pt, VA, 49 pp

Dronkers, J. J. 1964 *Tidal Computations in Rivers and Coastal Waters*. Amsterdam: North Holland Publishing Company, 516 pp.

Friedrichs, C. T. & Aubrey, D. G. 1988 Nonlinear tidal distortion in shallow well-mixed estuaries: a synthesis. *Estuarine, Coastal and Shelf Science* **27**, 521–545.

Fry, V. A. 1987. Tidal velocity asymmetry and bedload sediment transport in shallow embayments. MSc thesis, WHOI Technical Report No. 87–51, Woods Hole, MA, 55 pp.

Gallagher, B. S. & Munk, W. H. 1971 Tides in shallow water: Spectroscopy. *Tellus* **23**, 346–363.

Kabbaj, A. & LeProvost, C. 1980 Nonlinear tidal waves in channels: a perturbation method adapted to the importance of quadratic bottom friction. *Tellus* **32**, 143–163.

Kreiss, H. 1957 Some remarks about nonlinear oscillations in tidal channels. *Tellus* **9**, 53–68.

Meyer-Peter, E. & Müller, R. 1948 Formulas for bedload transport. *Proceedings 2nd Meeting, Mtl Association of Hydraulic Structure Research*, Appendix 2, pp. 39–64.

Roache, P. J. 1972 *Computational Fluid Dynamics*. Albuquerque: Hermosa Publishers, 434 pp.

Speer, P. E. & Aubrey, D. G. 1985 A study of non-linear tidal propagation in shallow inlet/estuarine systems. Part II: Theory. *Estuarine, Coastal and Shelf Science* **21**, 207–224.

Speer, P. E. 1984 Tidal distortion in shallow estuaries. PhD thesis, WHOI–MIT Joint Program in Oceanography, Woods Hole, MA, 210 pp.

Tee, K. T. 1976 Tide-induced residual current, a 2-D nonlinear numerical tidal model. *Journal of Marine Research* **34**, 603–628.

Wilson, K. C. 1966 Bed-load transport at high shear stress. *Journal of the Hydraulics Division, American Society of Civil Engineers* **92**, (HY6), 49–65.

Zimmerman, J. T. F. 1981 Dynamics, diffusion and geomorphological significance of tidal residual eddies. *Nature* **290**, 549–555.